Gain-Bandwidth Limitations and Synthesis of Single-Stub Bandpass Transmission-Line Structures

M. E. MOKARI-BOLHASSAN, MEMBER, IEEE, AND WALTER H. KU, MEMBER, IEEE

Abstract—**Gain-bandwidth limitations and synthesis of a class of bandpass transmission-line structures with a single shunted stub and n cascaded commensurate lines are presented in this paper. With a shunt shorted stub as the reactive constraint, the optimum gain bandwidth is derived for an ideal bandpass gain characteristic. Explicit gain-bandwidth and synthesis results have been obtained for the class of single-stub cascaded line structures with one and two cascaded lines for both maximally flat and Chebyshev characteristics. For the general case of n cascaded lines approximate gain-bandwidth limitations have also been derived. The explicit results including gain-bandwidth limitations and element values can be used for the design of this class of bandpass transmission-line networks for broad-band matching of the reactive constraint as well as impedance transformation.**

I. Introduction

THE SYNTHESIS of cascaded line structures with a single stub is well known [1]–[5]. The necessary and sufficient conditions for the realizability of such structures may be stated as follows. A given transmission scattering function $s_{12}(j\beta l)$ (where β is the propagation constant and l is the line length) is realizable as cascaded commensurate lines and a single stub if and only if, under the transformation,

$$\Omega = \tan \beta l \tag{1}$$

the amplitude function is rational, and $|s_{12}|^2$ is of the form

$$|s_{12}(j\Omega)|^2 = \frac{K\Omega^2(1+\Omega^2)^n}{P_{n+1}(\Omega^2)} \tag{2}$$

where n is the number of cascaded lines, P_{n+1} is an even function of degree $2(n+1)$ in Ω, and

$$0 < |s_{12}(j\Omega)|^2 \leq 1, \qquad \text{for } \Omega^2 > 0. \tag{3}$$

We may approximate a desired bandpass characteristic subject to these constraints. Analytical functions are available to approximate ideally flat gain responses in the maximally flat [1] or equiripple sense [2], [3].

The advantages of these structures are many. They provide a true bandpass characteristic with no transmission at dc. The stub can be used to adjust the resistor ratio of the load to the generator without altering the transmission

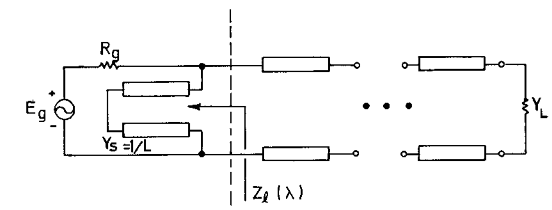

Fig. 1. General single-stub cascaded structure used to derive gain-bandwidth limitations.

characteristics [2], [3]. This type of structure is useful in broad-band matching a resistor shunted by a short-circuited transmission line, such loads are encountered in microwave absorbers, IMPATT diodes, and some antennas.

The gain-bandwidth restrictions for this structure viewed as a load and shown in Fig. 1 are obtained for both Butterworth and Chebyshev functions. The integral constraint for the load shown in Fig. 1 is given by [2], [6], [7]

$$\int_0^\infty \frac{1}{\Omega^2} \ln \frac{1}{|s_{11}|^2}\, d\Omega = \frac{2\pi}{R_g Y_s} - P. \tag{4}$$

Explicit relations are obtained for the $n = 1$ case. The graph and tables obtained for $n = 1$ and $n = 2$ are presented and are compared with restrictions obtained for ideal gain characteristics. Finally the results on the adjustment of the source-to-load resistance ratio by Carlin and Kohler [2] are extended for gain factors of $0 < K < 1$.

II. Butterworth Approximation

A function approximating single-stub bandpass characteristics in the maximally flat sense is given by [1]

$$P_{BP} = 1 + \varepsilon^2 \frac{\left[\frac{(1+\cot^2\theta_c)^{n/2}}{\cot^{n+1}\theta_c}\cot^{n+1}\theta\right]^2}{[1+\cot^2\theta]^n} \tag{5}$$

where

$$x = \alpha\cos\theta \qquad \Omega = \tan\theta \qquad \varepsilon^2 = (10^{\alpha_m/10} - 1) \tag{6}$$

and α_m is the insertion loss in decibels at the cutoff frequency θ_c/τ corresponding to $|x| = 1$. The parameter α determines the bandwidth [2], [3]. Substituting from (6) into (5) results in

$$|s_{12}|^2 = \frac{K}{P_{BP}} = \frac{K\Omega^2(1+\Omega^2)^n}{P_{n+1}(\Omega^2)} \tag{7}$$

which is realizable using commensurate line techniques

Manuscript received June 16, 1975; revised April 29, 1977. This work was supported in part by the National Science Foundation under Grant GK-31012X and in part by the Research Council of Pahlavi University.
M. E. Mokari-Bolhassan is with the Department of Electrical Engineering, Pahlavi University, Shiraz, Iran.
W. H. Ku is with the School of Electrical Engineering, Cornell University, Ithaca, NY 14853.

[1]–[3]. Here the gain factor K is a positive number less than unity which will be used for reactance absorption adjustment.

To find the allowable Y_s (see Fig. 1) for a given number of cascades n, bandwidth α, gain factor K, and the ripple factor ε, the integral relation of (4) is applied to this class of functions. For lossless structures we have

$$|s_{11}|^2 = 1 - |s_{12}|^2 = 1 - \frac{K\Omega^2(1+\Omega^2)^n}{\Omega^2(1+\Omega^2)^n + \mu^2}$$

or

$$|s_{11}|^2 = \frac{(1-K)\Omega^2(1+\Omega^2)^n + \mu^2}{\Omega^2(1+\Omega^2)^n + \mu^2} \tag{8}$$

where

$$\mu^2 = (10^{\alpha_m/10} - 1)(\alpha^2 - 1). \tag{9}$$

Substituting this in (4) gives

$$Q = \int_0^\infty \frac{1}{\Omega^2} \ln \frac{\Omega^2(1+\Omega^2)^n + \mu^2}{(1-K)\Omega^2(1+\Omega^2)^n + \mu^2} d\Omega = \frac{2\pi}{R_g Y_s}. \tag{10}$$

One needs to integrate this to find Y_s, which is, in general, impractical for $n > 1$.

An alternate method is due to Youla [7]. The polynomials in

$$s_{11}(\lambda)s_{11}(-\lambda) = \frac{-(1-K)\lambda^2(1-\lambda^2)^n + \mu^2}{-\lambda^2(1-\lambda^2)^n + \mu^2} \tag{11}$$

must be factored using numerical techniques. For $n = 1$ it is easy to factor out (11) in the λ domain. The gain-bandwidth restriction using either the integral constraint of (10) or the coefficient relations due to Youla is obtained as

$$\frac{1}{R_g Y_s} \geq \frac{1}{2\mu}\{\sqrt{1+2\mu} - \sqrt{(1-K+2\mu\sqrt{1-K})}\}, \quad \text{for } 0 < K \leq 1 \tag{12}$$

where μ is given in (9) in terms of the tolerance α_m and bandwidth parameter α. For $n = 2$, $s_{11}(\lambda)$ can be easily obtained from (11). In general it is of the form

$$s_{11}(\lambda) = -(1-K)^{1/2} \frac{\lambda^3 + b_2\lambda^2 + b_1\lambda + b_0}{\lambda^3 + a_2\lambda^2 + a_1\lambda + a_0}. \tag{13}$$

The gain-bandwidth restriction is obtained in the form

$$R_g Y_s \leq \frac{2\left[1 + (1-K)^{1/2}\dfrac{b_0}{a_0}\right]}{(1-K)^{1/2}\dfrac{b_1 a_0 - b_0 a_1}{a_0^2}}. \tag{14}$$

III. Chebyshev Approximation

The insertion gain function having only one zero of transmission at dc is given by [2]

$$|s_{12}|^2 = \frac{K}{1 + \varepsilon^2 \cos^2(n\phi + \xi)} \tag{15}$$

where

$$x = \cos\phi = \alpha\cos\theta$$

$$\cos\xi = x\sqrt{\frac{\alpha^2-1}{\alpha^2-x^2}}$$

$$\Omega = \tan\theta \tag{16}$$

and

$$\cos^2(n\phi+\xi) = \left[\frac{(\sqrt{\alpha^2+1}-\alpha)\,x\,T_n(x) + \alpha T_{n+1}(x)}{\sqrt{\alpha^2-x^2}}\right]^2 \tag{17}$$

for $n = 1$,

$$|s_{12}|^2 = \frac{K(\Omega^2+\Omega^4)}{\varepsilon^2\{\alpha(\sqrt{\alpha^2-1}+\alpha)-1\}^2 + \{1+2\varepsilon^2[-\alpha(\sqrt{\alpha^2-1}+\alpha)+1]\}\Omega^2 + (1+\varepsilon^2)\Omega^4} \tag{18}$$

and

$$|s_{11}|^2 = \frac{\varepsilon^2\{\alpha(\sqrt{\alpha^2-1}+\alpha)-1\}^2 + \{1-K+2\varepsilon^2(-\alpha(\sqrt{\alpha^2-1}+\alpha)+1)\}\Omega^2 + (1-K+\varepsilon^2)\Omega^4}{\varepsilon^2\{\alpha(\sqrt{\alpha^2-1}+\alpha)-1\}^2 + \{1+2\varepsilon^2(-\alpha\sqrt{\alpha^2-1}+\alpha)+1\}\Omega^2 + (1+\varepsilon^2)\Omega^4}. \tag{19}$$

Gain-bandwidth restriction is applied to this case ($n = 1$) and the explicit result is obtained as

$$\frac{1}{R_g Y_s} > \frac{1}{2\varepsilon y}\{\sqrt{1-2\varepsilon^2 y + 2\varepsilon y\sqrt{1+\varepsilon^2}} - \sqrt{1-K-2\varepsilon^2 y + 2\varepsilon y\sqrt{1-K+\varepsilon^2}}\}, \quad \text{for } 0 < K \leq 1 \tag{20}$$

where

$$y = [\alpha(\sqrt{\alpha^2-1}+\alpha)-1] > 0. \tag{21}$$

For $n = 1$, we can also factor out the reflection function in the λ domain; but the explicit relations are not obtained. Setting $n = 2$ in (15) and (19) results in

$$\cos^2(2\phi+\xi) = \frac{[(\sqrt{\alpha^2-1}-\alpha)^2(2\alpha^2-1-\Omega)^2 + \alpha^2(4\alpha^2-3-3\Omega^2)^2 + 2\alpha(\sqrt{\alpha^2-1}-\alpha)(2\alpha^2-1-\Omega^2)(4\alpha^2-3-3\Omega^2)]}{\Omega^2(1+\Omega^2)^2}. \tag{22}$$

TABLE I
NORMALIZED ELEMENT VALUES FOR A ONE-LINE ONE-STUB CHEBYSHEV MATCHING NETWORK WITH $\alpha = 2$ (OCTAVE BANDWIDTH)

		RIPPLE PARAMETER ε^2					
K		0.01	0.02	0.04	0.08	0.16	0.32
0.80	Y_{S1}	1.96257	2.55765	3.26547	4.10189	5.11696	6.42372
	Y_{01}	2.22128	2.06897	1.90664	1.75935	1.65942	1.64256
	Y_L	1.84358	1.56554	1.27598	1.00668	0.78328	0.61722
0.85	Y_{S1}	1.74775	2.27002	2.89049	3.62706	4.53059	5.70747
	Y_{01}	1.89938	1.76586	1.62732	1.50623	1.43139	1.43167
	Y_L	1.55346	1.31030	1.06224	0.83630	0.65243	0.51770
0.90	Y_{S1}	1.53719	1.98803	2.52398	3.16592	3.96550	5.02130
	Y_{01}	1.58930	1.47484	1.36073	1.26709	1.21691	1.23381
	Y_L	1.27239	1.06410	0.85759	0.67465	0.52923	0.42428
0.95	Y_{S1}	1.31137	1.68641	2.13550	2.68377	3.38233	4.31872
	Y_{01}	1.26787	1.17560	1.09004	1.02736	1.00417	1.03767
	Y_L	0.97745	0.80825	0.64802	0.51174	0.40641	0.33129
1.0	Y_{S1}	0.87763	1.13651	1.46390	1.88431	2.43746	3.18714
	Y_{01}	0.75012	0.71571	0.69061	0.68128	0.69619	0.74722
	Y_L	0.46083	0.38641	0.32054	0.26554	0.22217	0.18992

TABLE II
NORMALIZED ELEMENT VALUES FOR A TWO-LINE ONE-STUB BUTTERWORTH MATCHING NETWORK WITH A STUB AT THE INPUT AND $\alpha = 2$ (OCTAVE BANDWIDTH)

		RIPPLE PARAMETER ε^2					
K		0.01	0.04	0.02	0.16	0.25	0.36
0.80	Y_{S1}	1.97399	3.16501	4.01176	4.67588	5.22721	5.70182
	Y_{01}	2.14525	1.80231	1.58706	1.43834	1.32821	1.24257
	Y_{02}	1.68939	1.13784	0.84667	0.67077	0.55385	0.47107
	Y_L	1.62360	1.04347	0.74510	0.56937	0.45540	0.37628
0.85	Y_{S1}	1.75284	2.79032	3.52407	4.09854	4.57514	4.98533
	Y_{01}	1.83192	1.53178	1.34622	1.21892	1.12503	1.05220
	Y_{02}	1.41987	0.94497	0.69926	0.55226	0.45519	0.38658
	Y_L	1.36020	0.86172	0.61089	0.46479	0.37067	0.30563
0.90	Y_{S1}	1.53553	2.42132	3.04377	3.53008	3.93325	4.28018
	Y_{01}	1.52978	1.27139	1.11472	1.00819	0.93001	0.86955
	Y_{02}	1.15917	0.75956	0.55811	0.43906	0.36102	0.30610
	Y_L	1.10524	0.68705	0.48253	0.36508	0.29007	0.23854
0.95	Y_{S1}	1.30106	2.02209	2.52425	2.91553	3.23966	3.51854
	Y_{01}	1.21525	1.00115	0.87495	0.79022	0.72847	0.68092
	Y_{02}	0.88592	0.56715	0.41250	0.32273	0.26447	0.22374
	Y_L	0.83756	0.50578	0.35053	0.26287	0.20772	0.17015
1.00	Y_{S1}	0.65639	0.93385	1.12075	1.26557	1.38564	1.48923
	Y_{01}	0.59081	0.47462	0.41370	0.37448	0.34641	0.32497
	Y_{02}	0.27987	0.15993	0.1154	0.08551	0.06928	0.05821
	Y_L	0.22440	0.11355	0.07269	0.05214	0.04000	0.03209

Substituting (22) in

$$|s_{11}|^2 = \frac{(1-K) + \varepsilon^2 \cos^2(n\phi + \xi)}{1 + \varepsilon^2 \cos^2(n\phi + \xi)} \tag{23}$$

we obtain

$$|s_{11}(j\Omega)|^2 = \frac{\{(1-K)\Omega^6 + [2(1-K) + \varepsilon^2(\sqrt{\alpha^2-1} + 2\alpha)^2]\Omega^4 + \{1 - K + 2\varepsilon^2[-6\alpha^4 + 7\alpha^2 - 1 + 2\alpha\sqrt{\alpha^2-1} \cdot (-3\alpha^2+2)]\}\Omega^2 + \{\varepsilon^2[\sqrt{\alpha^2-1}(2\alpha^2-1) + 2\alpha^3 - 2\alpha]^2\}\}}{\{\Omega^6 + [2 + \varepsilon^2(\sqrt{\alpha^2-1} + 2\alpha)^2]\Omega^4 + \{1 + 2\varepsilon^2[-6\alpha^4 + 7\alpha^2 - 1 + 2\alpha\sqrt{\alpha^2-1}(-3\alpha^2+2)]\}\Omega^2 + \varepsilon^2[\sqrt{\alpha^2-1}(2\alpha^2-1) + 2\alpha^3 - 2\alpha]^2\}\}}. \tag{24}$$

The rest of the derivation is similar to the Butterworth case.

For large n we have to evaluate $|s_{11}(j\Omega)|^2$ depending on n and the type of response. Then the integral constraint may be applied directly to $|s_{11}|^2$, but there is no general solution available and each n needs separate treatment. One may also factor out $|s_{11}|^2$ into $s_{11}(\lambda)s_{11}(-\lambda)$ and then use the gain-bandwidth relations of Youla [7].

The gain-bandwidth relations obtained in the last sections are applied to $n = 1$ and $n = 2$ for Butterworth and Chebyshev approximations. Since $s_{11}(\lambda)s_{11}(-\lambda)$ has been factored in order to apply gain-bandwidth restrictions, it is a simple matter to synthesize $s_{11}(\lambda)$ further to realize the other elements in the circuit. This is performed for the octave bandwidth and the results are shown in Tables I–III.

Reactance absorption for different bandwidths is determined using the gain-bandwidth restrictions and the results are compared with those of ideal-gain characteristics in the next section. It should be noted that once Y_s is determined the generator impedance is easily obtained from

$$g_L = K\alpha^2 R_g Y_s^2/(4\varepsilon^2 f(\alpha)) \tag{25}$$

where

$$f(\alpha) = \alpha^{2(n+1)}(\alpha^2 - 1) \tag{26}$$

for the Butterworth approximation and

$$f(\alpha) = \tfrac{1}{4}(2\alpha)^{2(n+1)}(\alpha^2 - 1) \tag{27}$$

for the Chebyshev approximation.

Some observation is made in the following before we apply gain-bandwidth restrictions to ideal-gain characteristics.

a) The lowest value of Y_s corresponds to $K = 1$. If we need to absorb higher Y_s, we may do so either by decreasing K or increasing ε.

b) The maximum resistor ratio obtainable is the largest for $K = 1$ and as ε increases the resistor ratio also increases.

These two observations are theoretically predicted as will be discussed later in following sections.

c) For $n = 1$, Y_{01} is very close to normalized $Y_s = 1.0$, thus making the realization practical.

d) For $n = 2$, Y_{01} and Y_{02} do not spread too much for the Butterworth case, but the spread is very high for the Chebyshev case. Thus Butterworth results may be practically easier to realize.

TABLE III
NORMALIZED ELEMENT VALUES FOR A TWO-LINE ONE-STUB CHEBYSHEV MATCHING NETWORK WITH A STUB AT THE INPUT AND $\alpha = 2$ (OCTAVE BANDWIDTH)

		RIPPLE PARAMETER ε^2					
K		0.01	0.04	0.09	0.16	0.25	0.36
0.80	Y_{S1}	3.79583	5.00563	5.83046	6.55919	7.27133	7.99286
	Y_{01}	1.47093	1.21099	1.13029	1.11725	1.13889	1.18140
	Y_{02}	0.63969	0.34725	0.25168	0.20990	0.18976	0.18031
	Y_L	0.49514	0.21527	0.12980	0.09241	0.07268	0.06098
0.85	Y_{S1}	3.31119	4.35534	5.08705	5.74731	6.39885	7.06084
	Y_{01}	1.25032	1.03657	0.97595	0.97239	0.99779	1.04050
	Y_{02}	0.52574	0.28665	0.21015	0.17742	0.16216	0.15549
	Y_L	0.40033	0.17315	0.10499	0.07538	0.05980	0.05057
0.90	Y_{S1}	2.83305	3.72021	4.36818	4.96773	5.56499	6.17139
	Y_{01}	1.03946	0.87156	0.83094	0.83566	0.86566	0.90839
	Y_{02}	0.41734	0.22975	0.17147	0.14726	0.13653	0.13241
	Y_L	0.31030	0.13377	0.08197	0.05963	0.04788	0.04090
0.95	Y_{S1}	2.31578	3.04933	3.62316	4.16846	4.71343	5.26592
	Y_{01}	0.82409	0.70666	0.68769	0.70303	0.73522	0.77747
	Y_{02}	0.30709	0.17337	0.13365	0.11789	0.11153	0.10980
	Y_L	0.21885	0.09486	0.05952	0.04432	0.03626	0.03143
1.00	Y_{S1}	1.32930	1.92223	2.42612	2.90069	3.36505	3.82715
	Y_{01}	0.50551	0.47816	0.48853	0.51309	0.54547	0.58304
	Y_{02}	0.13921	0.09525	0.08188	0.07712	0.07609	0.07708
	Y_L	0.07591	0.03968	0.02809	0.02259	0.01946	0.01748

e) Finally, the rate of change in the element values becomes lower when ε increases beyond certain values.

It is usually a good practice to pick $K = 1$ for most of the applications unless some design specifications are not met. The increase in reactance absorption may not be justified if we have to increase the ripple factor beyond certain values predicted from the power match requirement and the tables.

IV. IDEAL-GAIN CHARACTERISTICS

Now we apply the integral constraint of (7) to the ideal-gain response shown in Fig. 2. For this ideal response (7) reduces to

$$\int_{\sqrt{\alpha^2-1}}^{\infty} \frac{1}{\Omega^2} \ln \frac{1}{1-K}\, d\Omega \le \frac{2\pi}{R_g Y_s}. \tag{28}$$

Integrating this leads to

$$K \le 1 - \exp\left(-2\pi\sqrt{\alpha^2-1}/R_g Y_s\right). \tag{29}$$

From this $\ln\{1/|s_{11}|_{\max}\}$ versus $\sqrt{\alpha^2-1}/R_g Y_s$ is plotted for the ideal case in Figs. 3 and 4, along with the same results for the $n = 1$ and the $n = 2$ case for different ripple factors ε^2 and the bandwidth parameter. These curves show that as ε^2 increases the reactance absorption increases and becomes very close to the ideal curves. It is also noted that as n increases from one to two the reactance absorption increases considerably closer to the optimal case. Therefore reactance absorption is usually achieved for small n's. Increasing n will result in a lower ripple parameter.

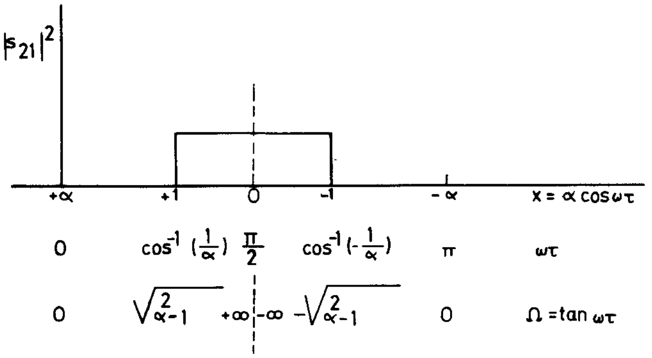

Fig. 2. Ideal-gain characteristics used to derive optimal gain-bandwidth relations.

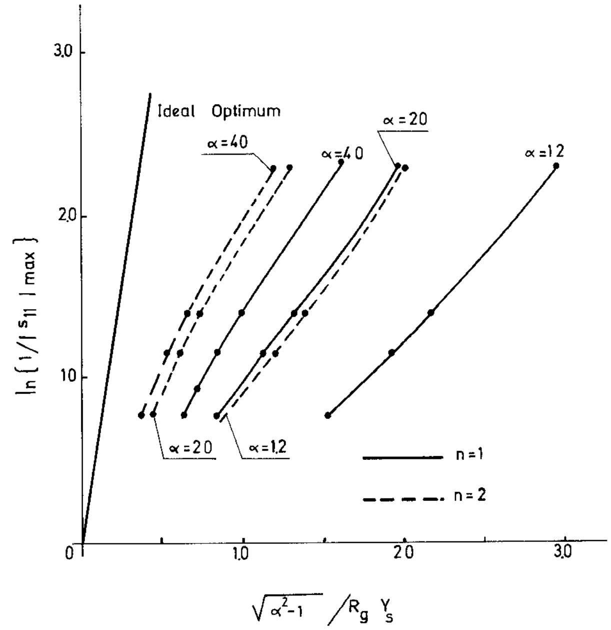

Fig. 3. Comparison of optimal reactance absorption with Chebyshev transfer functions with a ripple factor of $\varepsilon^2 = 0.01$.

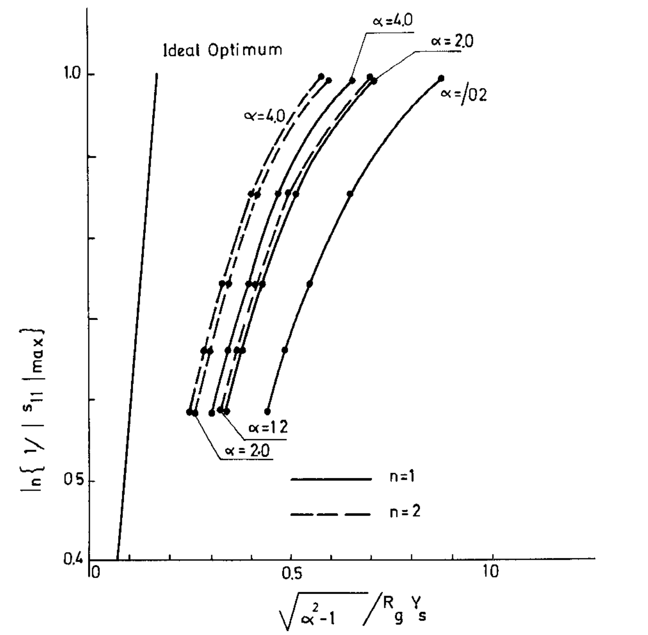

Fig. 4. Comparison of optimal reactance absorption with Chebyshev transfer function with a ripple factor of $\varepsilon^2 = 0.16$.

It should be pointed out here that the gain-bandwidth relations obtained here are not optimal in the sense of the ideal bandpass lumped domain response [8]. They are optimum for the case of the ideal periodic passband obtained using the $\Omega = \tan\theta$ transformation. Therefore, the results are valid for the comparison of an actual nth-order structure having periodic passbands with the ideal case.

VI. Conclusions

The gain-bandwidth relations for single-stub transmission-line structures have been investigated. The results are explicit for $n = 1$ for both Chebyshev and Butterworth approximations. The results for $n = 1$ and $n = 2$ are compared with the optimal reactance absorption curve for the ideal-gain response. As we decrease K or increase ε reactance absorption increases and the amount of the tradeoff involved is easily obtained from either the graphs or the tables.

The results of Carlin and Kohler [2] for resistor ratio adjustment for gain factor $K = 1$ have been extended for $0 < K \leq 1$. The results are also related for the reactance absorption properties of this type of structure.

Acknowledgment

The authors wish to thank Prof. H. J. Carlin of Cornell University for many helpful discussions and suggestions.

References

[1] E. M. T. Jones, "Synthesis of wide-band microwave filters to have prescribed insertion loss," *1956 IRE Convention Record*, pt. V, pp. 119–126.
[2] H. J. Carlin and W. Kohler, "Direct synthesis of band-pass transmission line structures," *IEEE Trans. Microwave Theory Tech.*, vol. MTT-13, May 1965.
[3] H. J. Carlin, "Distributed circuit design with transmission-line elements," *Proc. IEEE*, vol. 59, July 1971.
[4] G. Hoffman and H. Vanooteghem, "DISFIL, a computer program for optimum synthesis of TEM transmission-line filters," *IEEE Trans. Microwave Theory Tech.*, vol. MTT-20, p. 709, Oct. 1972.
[5] G. L. Matthaei, L. Young, and E. M. T. Jones, *Microwave Filters, Impedance Matching Networks, and Coupling Structures.* New York: McGraw-Hill, 1964.
[6] R. M. Fano, "Theoretical limitations on the broad-band matching of arbitrary impedances," *J. Franklin Institute*, vol. 249, pp. 57–83, Jan. 1950, also pp. 139–154, Feb. 1950.
[7] D. C. Youla, "A new theory of broad-band matching," *IEEE Trans. Circuit Theory*, vol. CT-11, pp. 30–50, Mar. 1964.
[8] H. J. Carlin and R. A. Friedenson, "Gain bandwidth properties of a distributed parameter load," *IEEE Trans. Circuit Theory*, vol. CT-15, pp. 455–464, Dec. 1968.

Letters

Noise Calibration Repeatability of an Airborne Third-Generation Radiometer

HANS-JUERGEN C. BLUME

Abstract—**A third-generation S-band radiometer has been calibrated at intervals over $3\frac{1}{2}$ years. The built-in stabilization concepts have proven to be very effective. In spite of some nonideal conditions (on runway, in wind, and in rain), an rms value of 0.7 K calibration repeatability has been observed with an average temperature deviation (bias error) of 0.03 K.**

Introduction

This third-generation radiometer is a 2.65-GHz (S-band) apparatus [1], which has been operated during about $3\frac{1}{2}$ years for about 400 h from aircraft or other elevated platforms. At intervals, the radiometer has been calibrated with a cryogenic noise source positioned in front of the antenna aperture. The measurement deviation from the temperature of the calibrated noise source represents an indication of the longtime stability of the overall characteristic of the radiometer. These deviations are presented and discussed for the $3\frac{1}{2}$ years of existence of the radiometer.

Manuscript received May 10, 1976; revised April 11, 1977.
The author is with NASA Langley Research Center, Hampton, VA 23665.

Calibration Procedures

A schematic representation of the calibration setup and the operation during calibration is shown in Fig. 1 in the form of a block diagram. As can be seen in Fig. 1 two concepts have been added to the first-generation Dicke radiometer [2]. The first concept consists in equalizing the temperature of the reference noise source at the second input of the Dicke switch with the temperature of the lossy microwave components between the antenna terminal and receiver input; once these temperatures are equalized they are kept extremely constant (± 0.03 K). The second concept consists in injecting pulsed portions from a constant noise source of higher noise power (avalanche diode) into the received noise power until the noise power of both Dicke-switch inputs is the same. The pulse frequency which determines the average value of the injected noise power is controlled by a feedback system. The pulse frequency is then a measure of the noise power (radiation) received by the antenna. In addition to eliminating both the time-consuming calibration cycles of the second-generation radiometer [3] and the noise effects of the microwave components, these two concepts also have the advantage of establishing longtime stability of the overall characteristic of the radiometer, in spite of gain variations, changes of losses, and other aging effects, as long as the noise source output power for noise injection remains constant. The ambient temperature of the noise source is stabilized to $\pm 1°$ C.